The Journal of Veterinary Medical Science

FULL PAPER

Anatomy

Immunohistochemical analysis for acetylcholinesterase and choline acetyltransferase in mouse cerebral cortex after traumatic brain injury

Tomoyo HORIO[1)], Aisa OZAWA[1)], Junichi KAMIIE[2)] and Motoharu SAKAUE[1)]*

[1)]Laboratory of Anatomy II, Department of Veterinary Medicine, School of Veterinary Medicine, Azabu University, Kanagawa 252-5201, Japan

[2)]Laboratory of Veterinary Pathology, Department of Veterinary Medicine, School of Veterinary Medicine, Azabu University, Kanagawa 252-5201, Japan

J. Vet. Med. Sci.
82(6): 827–835, 2020
doi: 10.1292/jvms.19-0551

Received: 8 October 2019
Accepted: 2 April 2020
Advanced Epub:
21 April 2020

ABSTRACT. The regulation of glial cells, especially astrocytes and microglia, is important to prevent the exacerbation of a brain injury because over-reactive glial cells promote neuronal death. Acetylcholine (ACh), a neurotransmitter synthesized and hydrolyzed by choline acetyltransferase (ChAT) and acetylcholinesterase (AChE), respectively, in the central nervous system, has the potential to regulate glial cells' states, i.e., non-reactive and reactive states. However, the expression levels of these ACh-related enzymes in areas containing reactive glial cells are unclear. Herein we immunohistochemically investigated the distributions of AChE and ChAT with reactive glial cells in the cryo-injured brain of mice as a traumatic brain injury model. Immunohistochemistry revealed AChE- and ChAT-immunopositive signals in injured areas at 7 days post-injury. The signals were observed in and around glial fibrillary acidic protein (GFAP)- or CD68-immunopositive cells, and the numbers of cells doubly positive for GFAP/AChE, GFAP/ChAT, CD68/AChE, and CD68/ChAT were significantly increased in injured areas compared to sham-operated areas. Enzyme histochemistry for AChE showed intensely positive signals in injured areas. These results suggest that reactive astrocytes and microglia express and secrete AChE and ChAT in brain-injury areas. These glial cells may adjust the ACh concentration around themselves through the regulation of the expression of ACh-related enzymes in order to control their reactive states.

KEY WORDS: acetylcholine, acetylcholinesterase, choline acetyltransferase, immunohistochemistry, traumatic brain injury

Traumatic brain injury (TBI) accounts for approximately 30% of the deaths due to trauma, and the number of patients experiencing a TBI is estimated at over 2.8 million per year in the USA [28]. Patients saved by surgery from a fatal outcome after a TBI often suffer from severe sequelae of their injury, and in some cases they have a shortened lifespan [26]. In head-impacting sports (e.g., rugby, boxing, and American football), athletes may suffer from chronic TBIs due to repeated impact and chronic mild traumatic injury to the brain. These athletes are reported to be at high risk of being affected by neurodegenerative diseases, Alzheimer's disease, Parkinson's disease, and amyotrophic lateral sclerosis [3]. Symptomatic treatments are the only choice for these patients after symptoms manifest, because there is no established treatment for the protection of surviving TBI patients and athletes whose condition is deteriorating.

Reactive glial cells contribute to the secondary diseases following a TBI [1, 7, 21]. Glial cells, i.e., astrocytes and microglia, in the central nervous system (CNS) are activated to proliferate, release inflammatory cytokines, phagocytose dead cells [15], form a glial scar to prevent the enlargement of the neuronal death area [23], and produce neurotrophic factors for axonal regeneration [2, 25]. Conversely, an over-activation of glial cells makes the glial cells over-proliferate and over-release inflammatory cytokines and reactive oxygen species, which induces further neuronal cell death [14, 19]. As these findings suggest the balance of the activation of astrocytes and microglia is not maintained in patients with TBIs, the control of balance between reactive and non-reactive glial cells may be a key point to prevent the secondary diseases in TBI patients.

The neurotransmitter acetylcholine (ACh) may regulate or contribute to the regulation of the reactivity of glial cells. ACh exerts its biological effects on cells via two types of ACh receptor: muscarinic ACh receptors and nicotinic ACh receptors. Nicotine, an agonist of nicotinic ACh receptors, suppresses the activation of astrocytes and microglia [11, 24]. ACh is synthesized and

*Correspondence to: Sakaue, M.: sakaue@azabu-u.ac.jp

hydrolyzed by choline acetyltransferase (ChAT) and acetylcholinesterase (AChE), respectively. Each type of ACh receptor has a specific affinity for ligand(s) and shows a specific expression level of each receptor, which determines biological activities. Synthesis and hydrolyzation of ACh can be the factors to determine the concentration of ACh, as ACh concentration is one of main factors to control the activities of the receptors. We thus hypothesized that (1) AChE and ChAT act as potent factors in the regulation of the activation of astrocytes and microglia via ACh hydrolysis and synthesis, and (2) AChE and ChAT could be targets for the regulation of glial cell activity. However, the distribution of AChE and ChAT and the ACh level in traumatic-injured brain have not been established.

We conducted the present study to determine the distribution of AChE and ChAT in the traumatic-injured brain containing reactive glia. To do so, we investigated the distribution of AChE and ChAT in cortical cryo-injury mice as a TBI model, using immunohistochemistry.

MATERIALS AND METHODS

Cryo-injury treatment

All protocols for this experiment were approved by the ethics committee for vertebrate experiments at Azabu University (ID# 160216-3). All surgical procedures were performed with the mice under deep anesthesia induced by isoflurane. Male C57BL/6Njcl mice (8 weeks old) were obtained from CLEA Japan (Tokyo, Japan). The cryo-injury treatment was performed by as described with minor modifications [27]. Briefly, after approximately 1 cm of skin of the mouse's head was incised at the median line and a cold stainless probe was completely chilled with liquid nitrogen, the cryo-injury was performed by placing the cold stainless probe (2 mm dia.) directly on the right parietal bone between the coronal suture and the bregma and approximately 3 mm lateral to the sagittal suture for 30 sec. The sham operation was performed by placing a stainless probe, room temperature, on the left parietal bone for 30 sec. Thereafter, the mice received food and water *ad libitum*. At day 7 after the cryo-injury and sham procedures, the mice were sacrificed, and the brain was removed as described below.

Preparation of frozen sections and fluorescence immunohistochemistry

On day 7 after the cryo-injury or sham treatment, seven mice were deeply anesthetized with pentobarbital sodium (Kyoritsu Seiyaku, Tokyo, Japan) and trans-cardially perfused with phosphate-buffered saline (PBS. pH 7.4) followed by 4% paraformaldehyde (PFA) in 0.1 M phosphate buffer (pH 7.4). The brain was removed and immersion-fixed for 48 hr on ice in the fixative. Fixed brains were cryoprotected by immersion in 30% sucrose in PBS for 48 hr at 4°C. Cryoprotected brains were embedded in O.C.T. compound (Sakura Finetek, Tokyo, Japan). Embedded tissue was quick-frozen and coronally sectioned in 10-μm slices with a cryostat (Leica Microsystems, Wetzlar, Germany).

The sections were subjected to heat-mediated antigen retrieval with citrate buffer (pH 6.0) for 15 min at 95°C. Sections were permeabilized with 0.1% Triton X-100 (v/v) in PBS, blocked with 2% goat serum (v/v; Sigma Aldrich, St. Louis, MO, USA) and 1% goat anti-mouse IgG (Jackson ImmunoResearch Lab, Philadelphia, PA, USA) in 0.1%TritonX-100 in PBS for 1 hr at room temperature. All incubations with primary antibodies were performed overnight at 4°C.

The primary antibodies and dilutions were as follows: rabbit monoclonal anti-NeuN antibody at 1:1,000 (cat.# ab177487, clone# EPR12763), rabbit monoclonal anti-glial fibrillary acidic protein (GFAP) antibody at 1:300 (cat.# ab68428, clone# EPR1034Y), rabbit polyclonal anti-CD68 antibody at 1:1,000 (cat.# ab125212), mouse monoclonal anti-CD68 at 1:1,000 (cat.# ab955), rabbit monoclonal anti-TMEM119 antibody at 1:300 (cat.# ab209064, clone#28–3), mouse monoclonal anti-AChE antibody at 1:1,000 (cat.# ab2803, clone#HR2), mouse monoclonal anti-ChAT antibody at 1:1,000 (cat.# ab35948, clone# 1E6), anti-myelin proteolipid protein (PLP) antibody at 1:2,000 (cat.# ab105784). Above primary antibodies are from Abcam (Cambridge, UK).

After being rinsed in PBS, the sections were incubated with Alexa 488-, 594- or 647-conjugated anti-mouse, -rabbit or -goat IgG (1:200, Jackson ImmunoResearch Lab), and counterstained with Hoechst 33258 (10 μg/m*l*, cat.# B2883, Sigma Aldrich). Other sections were processed without primary antibodies in parallel with each secondary antibody as negative controls.

Confocal imaging and analysis

Post-immunohistochemistry sections were observed (z-step size: 1.18 μm) by confocal microscopy (TCS SP5, Leica Microsystems). For a quantification analysis, three photomicrographs were randomly selected at the sites of cryo-injury treatment or sham operation per section. The three sections were randomly selected per the brain area showing the maximum diameter in the cryo-injured wound at the beginning, middle, and end of the area.

The numbers of cells with double-positive signals for the combination of GFAP/CD68/TMEM119 and/or ChAT/AChE were manually counted on photomicrographs, and we then calculated the rate of cells with a positive signal for ChAT/AChE among the cells with a positive signal for GFAP/CD68/TMEM119 per photomicrograph. The resulting data, tallied with the average of the rates from the individual values, are presented as the mean± standard deviation (SD) (%) in the Figures.

Enzyme histochemistry

To determine and estimate the existence of AChE and butyrylcholinesterase (BuChE) with each enzyme activity, we performed enzyme histochemistry using a modified Karnovsky-Roots method [4, 8]. The substrate used for the visualization of AChE activity was acetylthiocholine iodide, with which BuChE activity was inhibited by ethopropazine hydrochloride (Sigma Aldrich) at a final concentration of 0.06 mM.

Briefly, tissue sections were rinsed in 0.1 M of maleate buffer (pH 7.4) for 30 min and then incubated for 2 hr in 0.1 M maleate buffer (pH 6.8) containing 0.5 mM sodium citrate, 0.47 mM cupric sulfate, 0.05 mM potassium ferricyanide, 0.8 mM butyrylthiocholine iodide, and 0.4 mM acetylthiocholine iodide. The substrate used for the visualization of BuChE activity was butyrylthiocholine iodide, where AChE activity was inhibited by BW 284C51 (1,5-bis [4-allyl dimethylammonium phenyl] pentan-3-one dibromide, Sigma Aldrich) at 0.01 mM. All sections were then rinsed in distilled H_2O for 30 min and placed in 0.1% cobalt chloride in water for 10 min. After further rinsing in dH_2O, the sections were placed in phosphate buffer containing 1.39 mM 3,3′-diaminobenzidine tetrahydrochloride (DAB). After 5 min in the DAB solution, 50 μl of 0.15% H_2O_2 in dH_2O was added per m*l* of DAB solution, and the reaction was carried out for 15 min. The sections were then rinsed in dH_2O and coverslipped.

Western blot analysis

A mouse on day 7 after the cryo-injury and sham treatment was deeply anesthetized by intraperitoneal administration of sodium pentobarbital and euthanized by decapitation. Brain was immediately replaced and trimmed to separate cryo-injured and sham-operated areas. Pieces of the brain areas were homogenized in lysis buffer (50 mM Tris-HCL (pH 7.5), 250 mM NaCl, 5 mM EDTA, 0.1% Nonident P-40, 5 mM dithiothreitol, 10 mM NaF, 1 mM PMSF, 1 μg/m*l* aprotinin, and 1 μg/m*l* leupeptin). After centrifugation, the protein concentration in the supernatant was determined by a BCA assay (Bio-Rad, Hercules, CA, USA). SDS-polyacrylamide gel electrophoresis (SDS-PAGE) was performed with 25 μg of supernatant protein. For western blotting, proteins in the gel were transferred to a PVDF membrane (GE Healthcare, Buckinghamshire, UK) at 100 V for 2 hr. The membrane was rinsed with 0.05% Tween-20 PBS (T-PBS) and incubated in a blocking buffer, 1% bovine serum albumin in T-PBS, for 1 hr at room temperature. Then, mouse monoclonal anti-GFAP antibody (1:1,000, cat.# G3893, clone# G-A-5, Sigma-Aldrich) or mouse monoclonal anti-gryceraldehyde-3-phosphate dehydrogenase (GAPDH) antibody (1:2,000, cat.#MAB374, Sigma-Aldrich), as a primary antibody was reacted with the membrane for 12 hr at 4°C, followed by horseradish peroxidase-conjugated secondary antibody (goat anti-mouse IgG, 1:2,000, cat.#A4416, Sigma-Ardrich) for 1 hr at room temperature after rinsing in T-PBS. After rinsing the membranes, chemiluminescence enhanced on the membranes by ChemilumiOneTM (Nacalai Tesque, Kyoto, Japan) was determined by using RAS4000mini (GE Healthcare).

Imaging mass spectrometry

At 7 days after the cryo-injury, two mice were deeply anesthetized by an intraperitoneal administration of sodium pentobarbital and euthanized by exsanguination. Brains were immediately exposed and immersed in liquid nitrogen to rapidly freeze. The brains were then cryo-sectioned at 10 μm after trimming to remove crania and placed on glass slides. After the sections were dried, a CHCA (alpha-cyano-4-hydroxycinnamic acid) matrix solution was applied onto the surface of the sections. Matrix deposition was done using a solution of 5 mg/m*l* CHCA in 50% methanol with 0.05% trifluoroacetic acid (TFA) that we sprayed onto the tissue sections with the help of an automated pneumatic sprayer (TM-Sprayer, HTX Technologies, Chapel Hill, NC, USA). The nozzle distance was 46 mm, and the spraying temperature was set to 35°C. The matrix was sprayed (15 passes) over the tissue sections at a linear velocity of 700 mm/min with the flow rate set to 0.1 m*l*/min and the nitrogen pressure set at 10 psi. After each pass, a drying time of 40 sec was set on the spraying machine to give time for the sample to dry completely before the next pass.

A mass spectrometry analysis was performed on a MALDI LTQ Orbitrap XL mass spectrometer (Thermo Fisher Scientific, San José, CA, USA). Acetylcholine and choline were identified in the mass spectrometry by an ion at m/z 146.12 and 104.11, respectively. The signals of m/z 146.12 and 104.11 were detected with a MALDI ion trap. The evaluation of the spectra was performed with Xcalibur ver. 2.0.7. software, and the visualization of endogenous signals was achieved with ImageQuest™ software (both from Thermo Fisher Scientific).

Statistical analyses

All data are presented as the mean ± SD. The statistical analyses were performed using Statcel 3 software (OMS Publishing, Saitama, Japan). Comparisons between two independent means were performed using Student's *t*-test. Differences were considered significant at $P<0.05$.

RESULTS

We investigated neurons in the traumatic brain-injured area of the mice by immunohistochemistry using anti-NeuN antibody, a neuronal marker, to confirm whether the cryo-injury treatment adequately induced traumatic brain injury. There was no NeuN immunoreactivity in the central part of the traumatic-injured areas at 7 days after the cryo-injury, but NeuN-immunoreactive signals were observed in the cellular nuclei in the sham-operated brain areas and the peripheral part of the injured areas (Fig. 1A and 1B). These results confirmed the brain injury in the cryo-injured areas in the mouse model.

We investigated the distribution of AChE in the cryo-injured areas with immunohistochemistry and enzyme histochemistry. AChE immunoreactivity was intensely increased in the cryo-injured areas (Fig. 1D) compared to the sham-operated areas (Fig. 1C). Some positive signals looked like a large-granular vesicle. The enzyme histochemistry for AChE activity showed the intense positive signal of the enzyme activity in the injured areas compared to the sham-operated areas (Fig. 1E and 1F), whereas little positive signal of BuChE (a non-specific cholinesterase that hydrolyses many different choline-based esters) was detected by enzyme histochemistry in both the cryo-injured and sham-operated areas, and no difference was seen between these areas (data not shown).

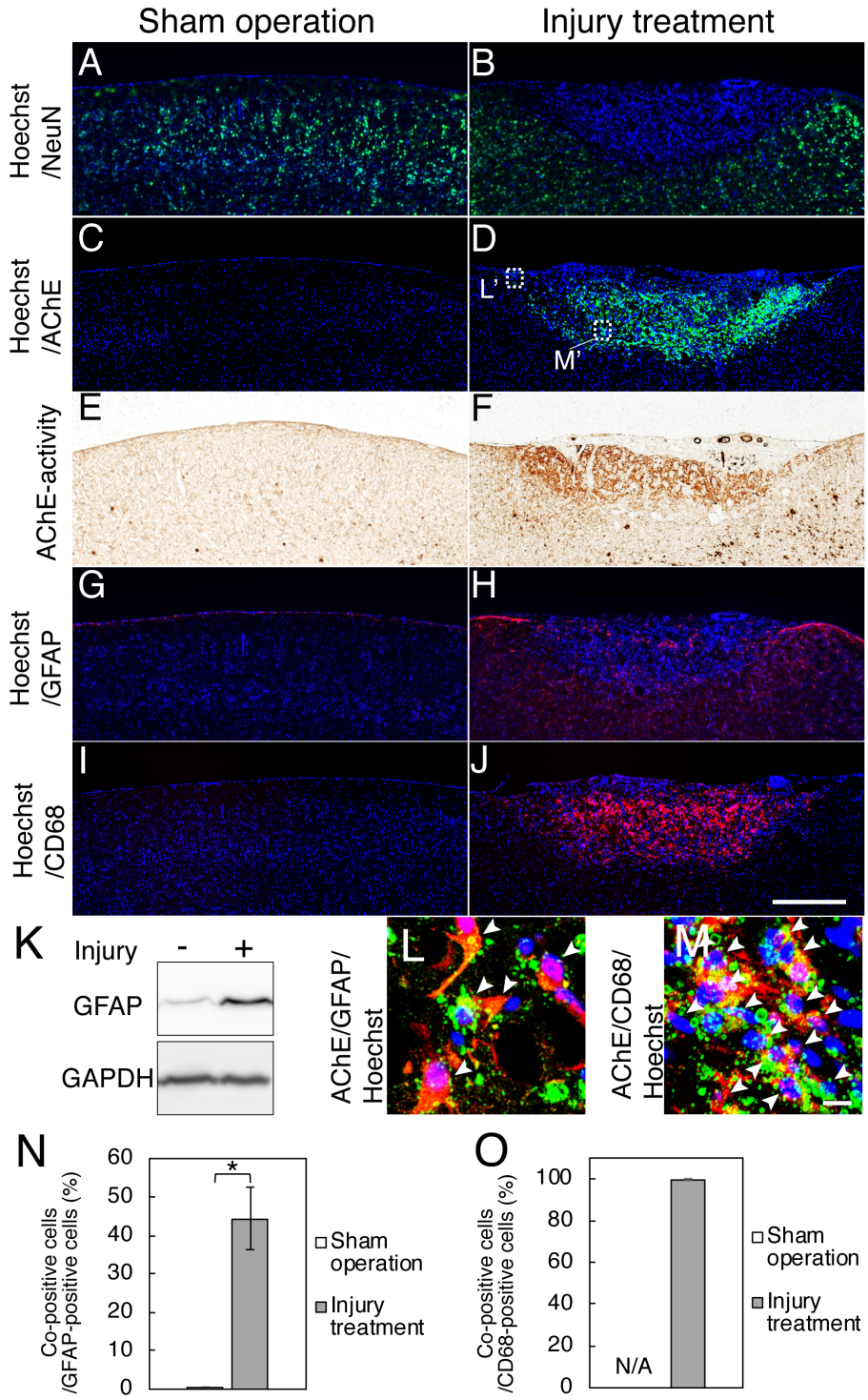

Fig. 1. Immunofluorescent staining for acetylcholinesterase (AChE), glial fibrillary acidic protein (GFAP), and CD68 in the injured areas of the murine traumatic brain injury (TBI) (cryo-injury) model. Fluorescence immunohistochemistry with anti-NeuN antibody (*green*; A and B), anti-AChE antibody (*green*; C and D), anti-GFAP antibody (*red*; G and H), and anti-CD68 antibody (*red*; I and J) in sham operation areas and cryo-injured areas of the brain. E and F: Enzyme activity of AChE (*brown*) in the brain areas shown by enzyme histochemistry. K: Western blot analysis for protein expression levels of GFAP and GAPDH. Protein samples from sham operation area (−) and cryo-injured area (+) were electrophoresed. Photomicrographs (L) and (M) show the magnified areas of *dotted-line squares* (L') and (M') in panel D, revealing the intracellular double expression of GFAP/AChE (L) and CD68/AChE (M). *Arrowheads*: Double-positive cells. All sections used in the fluorescent immunohistochemistry were counterstained with Hoechst 33258 (*blue*). Graphs (N) and (O) show the ratio (%) of AChE-positive cells among GFAP- or CD68-positive cells in the brain areas at 7 days after injury treatment (n=7), respectively. The numbers of cells were counted in three fields that were selected at random per section with a confocal microscope. The sections were also picked up at random three per area. **P*<0.05. Scale bars: 500 μm (A–J) or 10 μm (L and M).

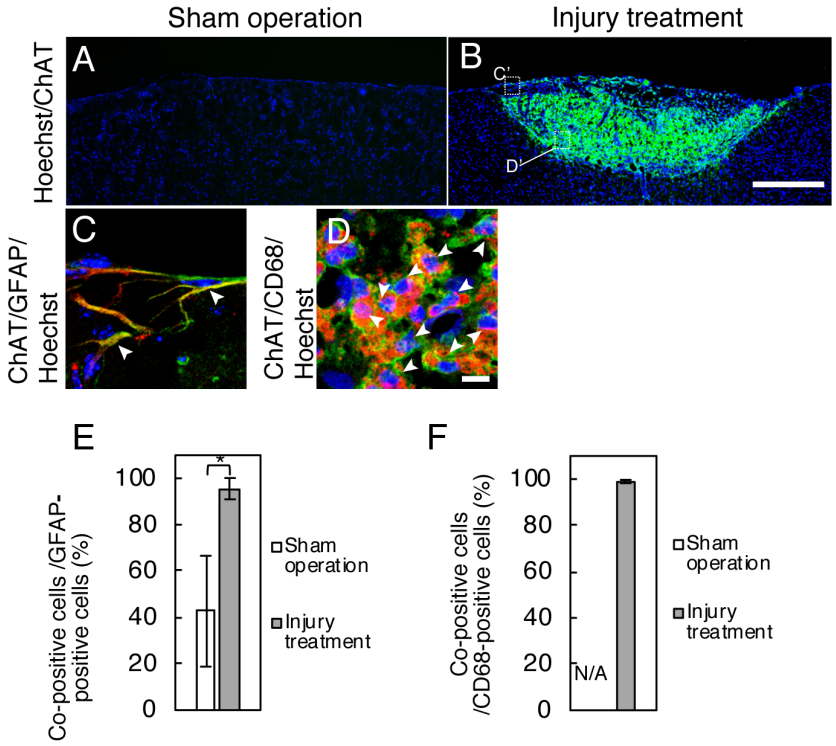

Fig. 2. Co-localization of choline acetyltransferase (ChAT)/glial fibrillary acidic protein (GFAP) or ChAT/CD68 in cryo-injured areas. A, B: Immunostaining shows the ChAT-immunopositive labeling (*green*). Double-immunostaining presents the co-localization of ChAT (*green*)/GFAP (*red*) (C) or ChAT (*green*)/CD68 (*red*) (D). Panels C and D are magnified figures of each part of the *dotted-line squares* (C') and (D') in panel B, respectively. Graphs: The rate of double-immunopositive cells for ChAT/GFAP to total GFAP-immunopositive cells (E) or ChAT/CD68 to CD68-immunoposive cells (F). *Arrowheads*: Double-positive cells. The data of double-immunopositive cells for ChAT/CD68 in sham-operated areas are not shown because no cell was immunolabeled for CD68 in those areas. All sections were counterstained with Hoechst 33258 (*blue*). Bars: 500 μm (A and B) or 10 μm (C and D).

To investigate the types of cells in the injured areas, we used antibodies against the cell marker proteins, GFAP, PLP and CD68, in an immunohistochemical analysis. Astrocytes are reactive and proliferate throughout a TBI [20]. GFAP is a maker protein for astrocytes and the expression is increased by activation of astrocytes. In sham-operated areas, immunopositive signals for GFAP were detected in the pia matter (Fig. 1G). The positive signal in the cerebral cortex parenchyma were not clearly observed at low magnification, but very-weak signals were found at high magnification (data not shown). The obviously immunopositive cells for GFAP were observed in the peripheral part of the cryo-injured areas (Fig. 1H), little the cells in the central part. We also performed immunohistochemistry for CD68, a marker of reactive microglia, because microglia are activated in brain injury [30]. Cells that were immunopositive for CD68 were detected predominantly in the central part of the cryo-injured areas (Fig. 1J) but not in the sham-operated areas (Fig. 1I) and the peripheral part of the cryo-injured areas (Fig. 1J). There was no immunoreactivity for PLP in the injured areas (data not shown). Western blot analysis for GFAP expression were used to determine whether astrocytes were activated in the cryo-injured areas. The result of the analysis showed that the GFAP-expression level of the cryo-injured areas was intensely increased compared to that of the sham-operated areas (Fig. 1K).

To identify whether the various types of cells were immunopositive for AChE, we performed immunohistochemistry for combinations of AChE/GFAP and AChE/CD68 in the peripheral or central parts of cryo-injured areas. In the central and peripheral parts of the injured areas, AChE immunoreactivity was detected in GFAP- and CD68-immunopositive cells, and in even the pericellular space (Fig. 1L and 1M). Most of the CD68-immunopositive cells showed immunoreactivity for AChE. Immunoreactivity for AChE and CD68 were also detected in nuclei. The value of double-immunopositive cells for AChE/GFAP relative to the number of GFAP-immunopositive cells was significantly increased to 44.44 ± 8.14% (Fig. 1N), and that for AChE/CD68 to the number of CD68-immunopositive cells was also significantly increased to 99.70 ± 0.39% (Fig. 1O) in the injured areas compared to the sham-operated areas ($P<0.05$). No double-immunopositive cells for AChE/GFAP or AChE/CD68 were detected in the sham-operated areas.

ACh is a substrate for AChE and is synthesized from choline and acetyl-CoA by ChAT. Our immunohistochemical analysis of ChAT detected intense immunoreactivity for ChAT in the cryo-injured areas (Fig. 2B) compared to the sham-operated areas (Fig. 2A). The immunohistochemical analyses for antibody combinations of ChAT/GFAP or ChAT/CD68 were performed to detect astrocytes or microglia, respectively, with the exclusion of neurons and oligodendrocytes. The immunopositive signals for ChAT were detected in GFAP-immunopositive cells (Fig. 2C) and in CD68-immunopositive cells of the cryo-injured areas (Fig. 2D). The

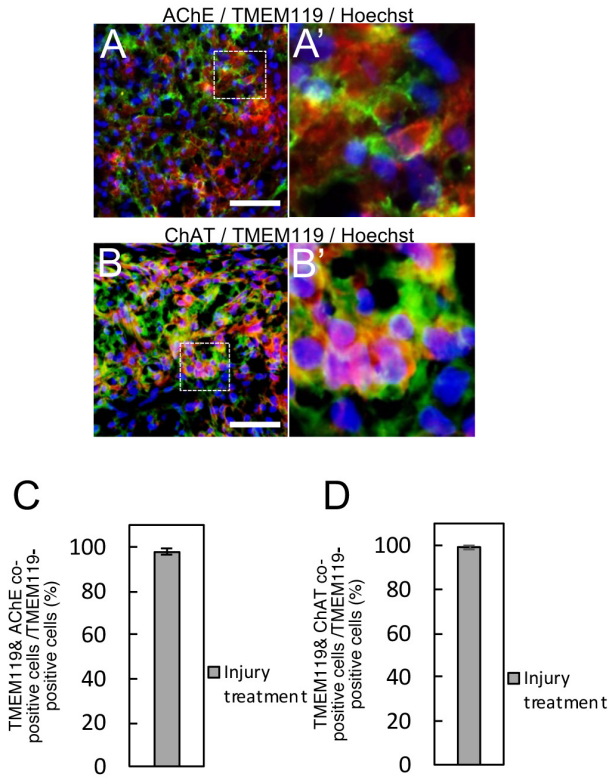

Fig. 3. Co-localization of acetylcholinesterase (AChE)/TMEM119 or choline acetyltransferase (ChAT)/TMEM119 in cryo-injured areas. Double-immunostaining presents the co-localization of immunopositive labelings for AChE (*green*)/TMEM119 (*red*) (A). Immunopositive labelings for ChAT (*green*) were overlapped that for TMEM119 (B). Photomicrographs (A') and (B') are the magnified area of dotted-line squares in panel (A) and (B), respectively. Bars: 40 μm. Graphs: the rate of co-immunopositive cells for AChE/TMEM119 (C) or ChAT/TMEM119 (D) to TMEM119-immunopositive cells. All sections were counterstained with Hoechst 33258 (*blue*).

ChAT-positive signals were also in the pericellular space of CD68-immunopositive cells, but not in that of GFAP-immunopositive cells. CD68 immunoreactivity was also detected in nuclei. In addition, the value of the cells that were double-immunopositive for ChAT/GFAP relative to the number of GFAP-immunopositive cells was significantly greater at 95.55 ± 4.57% in the cryo-injured areas compared to 42.63 ± 23.91% in the sham-operated areas (P<0.05; Fig. 2E), and the value for double-immunopositivity for ChAT/CD68 to the number of CD68-immunopositive cells was also greater at 98.99 ± 0.73% in the cryo-injured areas (Fig. 2F).

Immunohistochemistry for TMEM119, a specific marker for microglia, were also performed to identify AChE-immunopositive microglia because reactive macrophages migrated from peripheral blood also have immunoreactivity for CD68. Immunoreactivity for AChE was detected in TMEM119-immunopositive cells, so the co-immunopositive cells were considered to be microglia (Fig. 3A). The relative value of co-immunopositive cells for AChE/TMEM119 to the number of TMEM119-positive cells was 97.92 ± 1.44% (Fig. 3C). Further, almost all of TMEM119-immunopositive cells showed immunoreactivity for ChAT (Fig. 3B), and the relative value of co-immunopositive cells for ChAT was 99.05 ± 0.88% of TMEM119-immunopositive cells (Fig. 3D).

Immunoreactivity for ChAT was significantly detected in the cryo-injured areas, and we thus performed imaging mass spectrometry to determine the existence and distribution of ACh in cryo-injured brain because ACh is a product of ChAT and a substance that affects the conditions of glial cells [11, 24]. ACh signal was detected predominantly in injured areas but not in sham-operated areas (Fig. 4B). Choline signal extended over the cerebral cortex in both cryo-injured and sham-operated areas, but the signal was more heavily distributed in cryo-injured areas of the cerebral cortex than in the sham-operated areas (Fig. 4C).

DISCUSSION

Our present findings demonstrated the distributions of the ACh-related enzymes AChE and ChAT in a mouse model of TBI with cryo-injury treatment. Immunoreactivity for AChE was detected in GFAP-immunopositive and CD68-immunopostive cells in cryo-injured areas, and the enzyme histochemistry for AChE showed the positive labeling in cryo-injured areas, indicating that astrocytes and microglia expressed AChE in cryo-injured areas. Immunoreactivity for AChE was not observed in sham-operated areas. Since the GFAP immunoreactivity was intense, and CD68 and TMEM119 was detected in cryo-injured areas but not in sham-operated areas, we speculate that astrocytes and microglia increased the expression of AChE when these cells were activated. The reason why some immunolabelings for AChE were like a granular vesicle in cryo-injured areas is unknown.

GFAP is one of well-known astrocytic markers, i.e., vimentin, Pax6 and aldehyde dehydrogenase 1, and there are some subtypes of astrocytes. Expression patterns of the astrocytic markers were different for each subtype of astrocytes [10]. In the present study, we showed that the immunopositive astrocytes for GFAP were immunoreactive for AChE, however, we didn't perform immunohistochemistry for astrocytic markers except GFAP. It has been unclear the difference of ACh-related enzyme expressions for each subtype of astrocytes. Further experiments with antibodies for some astrocytic markers would be needed on identification

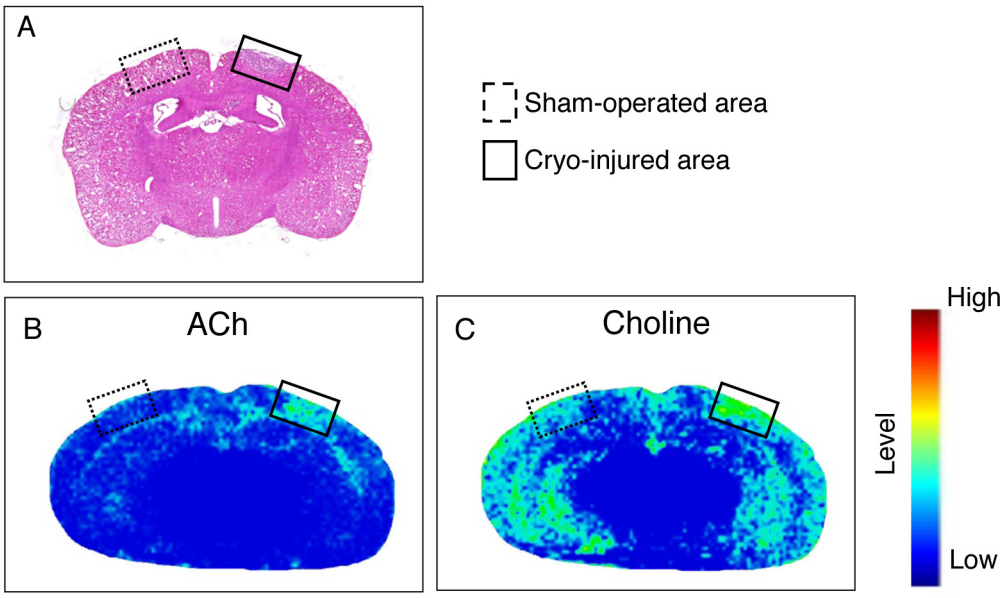

Fig. 4. Imaging mass spectrometry results for acetylcholine (ACh) and choline in cryo-injured areas. *Dotted-line squares*: Sham-operated areas. *Solid-line squares*: Cryo-injured areas. A: Image of a brain section stained with hematoxylin and eosin. Imaging results of derived ions from ACh (B) and choline (C) show the relative intensity.

of expression of ACh-related enzymes in subtypes of astrocytes including reactive astrocytes.

Our immunohistochemical analysis for ChAT revealed an increase in the immunolabeling in cryo-injured areas, and the immunopositive labeling was observed in GFAP-immunopositive and CD68-immunopositive cells in the injured areas, indicating that reactive astrocytes and microglia probably expressed ChAT themselves. The immunopositive labeling for ChAT was also detected around glial cells in cryo-injured areas. ChAT, a secretory protein that human astrocytes can secrete in primary culture, has the ability to produce ACh [29]. Our imaging mass spectrometry observation that ACh signal was present in cryo-injured areas supports the possibility that enzyme activity of the intracellular or extracellular ChAT exists in these injured areas. The enzyme may synthesize even around the glial cells in cryo-injured areas.

Increases in the levels of ACh and ChAT with reactive astrocytes and microglia may contribute to the control of the glial reactivity via ACh. Herein we observed that cryo-injury stimulated the activation of glial cells and increases in the ChAT and of ACh levels. These results suggest that the increase in the ChAT expression in and around glial cells may make the ACh level increase. Nicotine, an ACh agonist for nicotinic ACh receptors (AChRs), suppresses the reactivity of astrocytes and microglia via alpha7-nicotinic AChR [11, 21]. Astrocytes also express other nicotinic and muscarinic AChRs [6, 18, 22]. Thus, in areas with a surrounding high ACh level, a further reactivity of astrocytes and microglia was perhaps suppressed by ACh; however, adequate reactivity and the proliferation of glial cells are needed to protect the brain from an exacerbation and expansion of inflammation to outside the traumatic injured area [9, 12]. The level of ACh may be adequately controlled in order for the ACh to bind to appropriate AChRs for the induction of biological reactivity in glial cells. The induced GFAP expression in C6 cells was suppressed by an AChE inhibitor and siRNA for AChE [17, 18], which suggests that AChE dysfunction would induce an accumulation of ACh around glial cells and that ACh is an endogenous agonist for AChRs to control the condition of the glial cells.

AChE and CD68 immunoreactivity were also detected in nuclei of GFAP-immunopositive and CD68-immunopostive cells (Fig. 1L, 1M, and Fig. 2D). Du *et al.* have reported a nuclear translocation-dependent role for AChE as an apoptotic deoxyribonuclease [5]. Therefore, AChE may also play a role as an apoptotic deoxyribonuclease in astrocytes and microglia. CD68 is also localized in the nuclei of Glioblastoma cell lines [16], monocytes and macrophages [13]. These cells are involved in immune system. Although the role in the nucleus has been unknown with data in the present study, CD68 may regulate immune-related functions in nuclei.

In the present study, high levels of ACh and immunoreactivity for ChAT and AChE were detected in and around glial cells in the cryo-injured areas of the mouse brain. Taking these results together along with the high level of ACh synthesis by ChAT that is expressed in reactive astrocytes and microglia, the cells may locally inactivate ACh around themselves with AChE to provide the conditions for the maintenance of the glial cells' reactive status. The ACh level is conceivably coordinated by a balance between the enzyme activities of ChAT and AChE (Fig. 5). However, the ACh level around cells in the cryo-injured areas remains unknown despite our present observations. Investigations of the contribution of the local balance to the ACh level may help us better understand the function of ACh in the control of glial cells *in vivo*.

CONFLICT OF INTEREST. The authors declare that they have no conflict of interest.

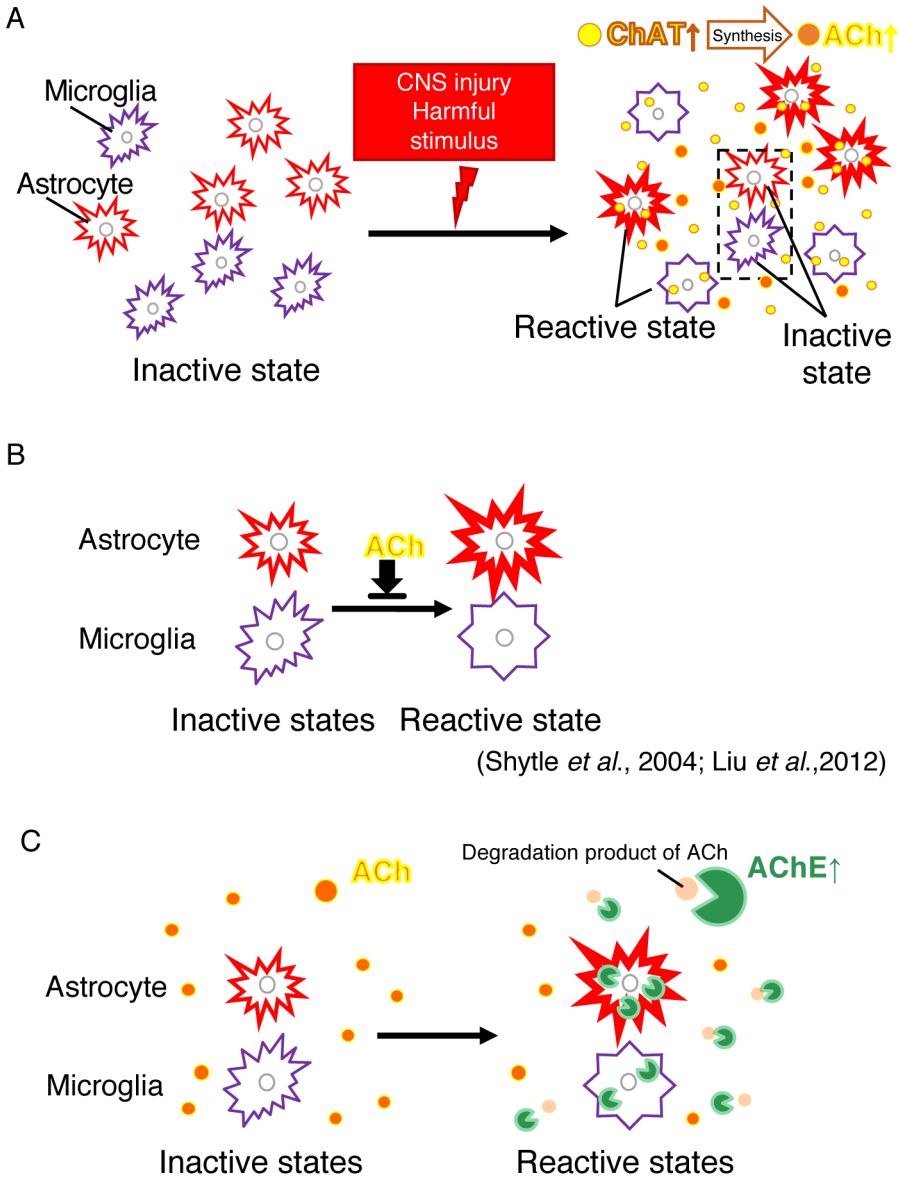

Fig. 5. Hypothesis regarding the regulation of astrocyte and microglial activation via acetylcholinesterase (AChE) and choline acetyltransferase (ChAT). (A) Glial activation and Acetylcholine (ACh) increase. Brain injury induces astrocyte and microglial activation, and then as the expression of ChAT from these cells increases (Figs. 2 and 3), the synthesis of ACh are increased (Fig. 4). (B) ACh agonists have been reported to suppress activation of astrocytes [11] and microglia [24]. (C) Effect of AChE on glial cells. AChE expression in/around astrocytes and microglia may adjust the ACh level to maintain adequate activation of the glial cells (Fig. 1).

ACKNOWLEDGMENT. This work was supported by JSPS KAKENHI, Grant-in-Aid for Scientific Research (C), Grant Number JP 17K08117.

REFERENCES

1. Acosta, S. A., Tajiri, N., Shinozuka, K., Ishikawa, H., Grimmig, B., Diamond, D. M., Sanberg, P. R., Bickford, P. C., Kaneko, Y. and Borlongan, C. V. 2013. Long-term upregulation of inflammation and suppression of cell proliferation in the brain of adult rats exposed to traumatic brain injury using the controlled cortical impact model. *PLoS One* **8**: e53376. [Medline] [CrossRef]
2. Chen, Z., Jalabi, W., Hu, W., Park, H. J., Gale, J. T., Kidd, G. J., Bernatowicz, R., Gossman, Z. C., Chen, J. T., Dutta, R. and Trapp, B. D. 2014. Microglial displacement of inhibitory synapses provides neuroprotection in the adult brain. *Nat. Commun.* **5**: 4486. [Medline] [CrossRef]
3. Cruz-Haces, M., Tang, J., Acosta, G., Fernandez, J. and Shi, R. 2017. Pathological correlations between traumatic brain injury and chronic neurodegenerative diseases. *Transl. Neurodegener.* **6**: 20. [Medline] [CrossRef]
4. Darreh-Shori, T., Vijayaraghavan, S., Aeinehband, S., Piehl, F., Lindblom, R. P., Nilsson, B., Ekdahl, K. N., Långström, B., Almkvist, O. and

Nordberg, A. 2013. Functional variability in butyrylcholinesterase activity regulates intrathecal cytokine and astroglial biomarker profiles in patients with Alzheimer's disease. *Neurobiol. Aging* **34**: 2465–2481. [Medline] [CrossRef]
5. Du, A., Xie, J., Guo, K., Yang, L., Wan, Y., OuYang, Q., Zhang, X., Niu, X., Lu, L., Wu, J. and Zhang, X. 2015. A novel role for synaptic acetylcholinesterase as an apoptotic deoxyribonuclease. *Cell Discov.* **1**: 15002. [Medline] [CrossRef]
6. Graham, A. J., Ray, M. A., Perry, E. K., Jaros, E., Perry, R. H., Volsen, S. G., Bose, S., Evans, N., Lindstrom, J. and Court, J. A. 2003. Differential nicotinic acetylcholine receptor subunit expression in the human hippocampus. *J. Chem. Neuroanat.* **25**: 97–113. [Medline] [CrossRef]
7. Impellizzeri, D., Campolo, M., Bruschetta, G., Crupi, R., Cordaro, M., Paterniti, I., Cuzzocrea, S. and Esposito, E. 2016. Traumatic brain injury leads to development of Parkinson's disease related pathology in mice. *Front. Neurosci.* **10**: 458. [Medline] [CrossRef]
8. Karnovsky, M. J. and Roots, L. 1964. A "direct-coloring" thiocholine method for cholinesterases. *J. Histochem. Cytochem.* **12**: 219–221. [Medline] [CrossRef]
9. Karve, I. P., Taylor, J. M. and Crack, P. J. 2016. The contribution of astrocytes and microglia to traumatic brain injury. *Br. J. Pharmacol.* **173**: 692–702. [Medline] [CrossRef]
10. Liddelow, S. A., Guttenplan, K. A., Clarke, L. E., Bennett, F. C., Bohlen, C. J., Schirmer, L., Bennett, M. L., Münch, A. E., Chung, W. S., Peterson, T. C., Wilton, D. K., Frouin, A., Napier, B. A., Panicker, N., Kumar, M., Buckwalter, M. S., Rowitch, D. H., Dawson, V. L., Dawson, T. M., Stevens, B. and Barres, B. A. 2017. Neurotoxic reactive astrocytes are induced by activated microglia. *Nature* **541**: 481–487. [Medline] [CrossRef]
11. Liu, Y., Hu, J., Wu, J., Zhu, C., Hui, Y., Han, Y., Huang, Z., Ellsworth, K. and Fan, W. 2012. α7 nicotinic acetylcholine receptor-mediated neuroprotection against dopaminergic neuron loss in an MPTP mouse model via inhibition of astrocyte activation. *J. Neuroinflammation* **9**: 98. [Medline] [CrossRef]
12. Loane, D. J. and Byrnes, K. R. 2010. Role of microglia in neurotrauma. *Neurotherapeutics* **7**: 366–377. [Medline] [CrossRef]
13. Luque, M. C., Gutierrez, P. S., Debbas, V., Kalil, J. and Stolf, B. S. 2015. CD100 and plexins B2 and B1 mediate monocyte-endothelial cell adhesion and might take part in atherogenesis. *Mol. Immunol.* **67** 2 Pt B: 559–567. [Medline] [CrossRef]
14. Marín-Teva, J. L., Cuadros, M. A., Martín-Oliva, D. and Navascués, J. 2011. Microglia and neuronal cell death. *Neuron Glia Biol.* **7**: 25–40. [Medline] [CrossRef]
15. Morizawa, Y. M., Hirayama, Y., Ohno, N., Shibata, S., Shigetomi, E., Sui, Y., Nabekura, J., Sato, K., Okajima, F., Takebayashi, H., Okano, H. and Koizumi, S. 2017. Reactive astrocytes function as phagocytes after brain ischemia via ABCA1-mediated pathway. *Nat. Commun.* **8**: 28. [Medline] [CrossRef]
16. Mukherjee, S., Baidoo, J., Fried, A., Atwi, D., Dolai, S., Boockvar, J., Symons, M., Ruggieri, R., Raja, K. and Banerjee, P. 2016. Curcumin changes the polarity of tumor-associated microglia and eliminates glioblastoma. *Int. J. Cancer* **139**: 2838–2849. [Medline] [CrossRef]
17. Ozawa, A., Kadowaki, E., Haga, Y., Sekiguchi, H., Hemmi, N., Kaneko, T., Maki, T., Sakabe, K., Hara, S., Yamamoto, M., Arishima, K. and Sakaue, M. 2013. Acetylcholine esterase is a regulator of GFAP expression and a target of dichlorvos in astrocytic differentiation of rat glioma C6 cells. *Brain Res.* **1537**: 37–45. [Medline] [CrossRef]
18. Ozawa, A., Kadowaki, E., Horio, T. and Sakaue, M. 2019. Acetylcholine suppresses the increase of glia fibrillary acidic protein expression via acetylcholine receptors in cAMP-induced astrocytic differentiation of rat C6 glioma cells. *Neurosci. Lett.* **698**: 146–153. [Medline] [CrossRef]
19. Phatnani, H. and Maniatis, T. 2015. Astrocytes in neurodegenerative disease. *Cold Spring Harb. Perspect. Biol.* **7**: a020628. [Medline] [CrossRef]
20. Ridet, J. L., Malhotra, S. K., Privat, A. and Gage, F. H. 1997. Reactive astrocytes: cellular and molecular cues to biological function. *Trends Neurosci.* **20**: 570–577. [Medline] [CrossRef]
21. Saing, T., Dick, M., Nelson, P. T., Kim, R. C., Cribbs, D. H. and Head, E. 2012. Frontal cortex neuropathology in dementia pugilistica. *J. Neurotrauma* **29**: 1054–1070. [Medline] [CrossRef]
22. Sharma, G. and Vijayaraghavan, S. 2002. Nicotinic receptor signaling in nonexcitable cells. *J. Neurobiol.* **53**: 524–534. [Medline] [CrossRef]
23. Shinozaki, Y., Shibata, K., Yoshida, K., Shigetomi, E., Gachet, C., Ikenaka, K., Tanaka, K. F. and Koizumi, S. 2017. Transformation of astrocytes to a neuroprotective phenotype by microglia via P2Y1 receptor downregulation. *Cell Rep.* **19**: 1151–1164. [Medline] [CrossRef]
24. Shytle, R. D., Mori, T., Townsend, K., Vendrame, M., Sun, N., Zeng, J., Ehrhart, J., Silver, A. A., Sanberg, P. R. and Tan, J. 2004. Cholinergic modulation of microglial activation by alpha 7 nicotinic receptors. *J. Neurochem.* **89**: 337–343. [Medline] [CrossRef]
25. Sidoryk-Wegrzynowicz, M., Wegrzynowicz, M., Lee, E., Bowman, A. B. and Aschner, M. 2011. Role of astrocytes in brain function and disease. *Toxicol. Pathol.* **39**: 115–123. [Medline] [CrossRef]
26. Strauss, D. J., Shavelle, R. M. and DeVivo, M. J. 1999. Life tables for people with traumatic brain injury. *J. Insur. Med.* **31**: 104–105.
27. Tatsumi, K., Haga, S., Matsuyoshi, H., Inoue, M., Manabe, T., Makinodan, M. and Wanaka, A. 2005. Characterization of cells with proliferative activity after a brain injury. *Neurochem. Int.* **46**: 381–389. [Medline] [CrossRef]
28. Taylor, C. A., Bell, J. M., Breiding, M. J. and Xu, L. 2017. Traumatic brain injury-related emergency department visits, hospitalizations, and deaths −United States, 2007 and 2013. *MMWR Surveill. Summ.* **66**: 1–16. [Medline] [CrossRef]
29. Vijayaraghavan, S., Karami, A., Aeinehband, S., Behbahani, H., Grandien, A., Nilsson, B., Ekdahl, K. N., Lindblom, R. P., Piehl, F. and Darreh-Shori, T. 2013. Regulated extracellular choline acetyltransferase activity- the plausible missing link of the distant action of acetylcholine in the cholinergic anti-inflammatory pathway. *PLoS One* **8**: e65936. [Medline] [CrossRef]
30. Xu, H., Wang, Z., Li, J., Wu, H., Peng, Y., Fan, L., Chen, J., Gu, C., Yan, F., Wang, L. and Chen, G. 2017. The polarization states of microglia in TBI: A new paradigm for pharmacological intervention. *Neural Plast.* **2017**: 5405104. [Medline] [CrossRef]